Heliyon 5 (2019) e02038

Contents lists available at ScienceDirect

Heliyon

journal homepage: www.heliyon.com

Density functional theory, molecular docking and bioassay studies on (*S*)-2-hydroxy-N-(2*S*,3*S*,4*R*,*E*)-1,3,4 trihydroxyicos-16-en-2-yl) tricosanamide

Taj Ur Rahman [a], Muhammad Aurang Zeb [b,*], De-Bing Pu [b], Wajiha Liaqat [c], Khurshid Ayub [d], Wei-Lie Xiao [b], Tariq Mahmood [d], Muhammad Sajid [e], Riaz Hussain [f]

[a] *Department of Chemistry, Mohi-Ud-Din Islamic University AJ&K, Pakistan*
[b] *Key Laboratory of Medicinal Chemistry for Natural Resource, Ministry of Education, School of Chemical Science and Technology, Yunnan University, Kunming, PR China*
[c] *Institute of Chemical Sciences, University of Peshwar, 25120, Pakistan*
[d] *COMSATS Institute of Information Technology, University Road, Tobe Camp, Abbottabad, KPK, 22060, Pakistan*
[e] *Department of Biochemistry, Hazara University, Mansehra, KPK, Pakistan*
[f] *Department of Chemistry, University of Education, Okara Campus, Okara, Punjab, Pakistan*

ARTICLE INFO

Keywords:
Natural product chemistry
Organic chemistry
Theoretical chemistry
Indigofera heterantha
Density functional theory
Electronic and spectroscopic properties
Molecular docking

ABSTRACT

A novel indigoferamide-A, earlier isolated from the seeds of *Indigofera heterantha* Wall was characterized using density functional theory, molecular docking and bioassays studies. Density functional theory calculations were performed at B3LYP/6-31G(d,p) to gain geometric insight of the compound. Conformational analyses have been performed around three important dihedral angles to explore the lowest energy structure and conformer. The simulated vibrational spectrum of the compound at B3LYP/6-31G(d,p) was scaled with two scaling factors, and the scaled harmonic vibrations shows nice correlation with the experimental values. ^{1}H and ^{13}C NMR chemical shifts were calculated using Cramer's re-parameterized function W04 at 6- 31G(d,p) basis set. Several conformers lying within 2 kcal mol^{-1} of the minimum energy conformer were considered; however, the chemical shifts were not significantly different among these conformers. The Gaussian averaged theoretical ^{1}H and ^{13}C chemical shifts correlate nicely with the experimental data. Electronic properties such as band gap, ionization potential and electron affinities were also simulated for the first time, however, no comparison could be made with the experiment. The compound was also screened for urease, antiglycation activities and the theoretical explanation of the results is provided based on molecular docking simulations.

1. Introduction

Indigofera heterantha Wall, generally known as *Indigo* Himalayan, is a deciduous shrub distributed in the tropical region of the globe. In Pakistan, 24 species of the genus are available [1]. Natural products such as flavonoids, lignin, alkaloids, steroids, triterpenes and acylphloroglucinols are the main compounds reported from the genus [2]. Other compounds like quinines, saponins, tannins, caffeic acid, gallic acid, rutin, myricetin, quercitrin and galangin were also isolated from the genus *Indigofera*. Some species of the genus contain 3- nitro propionate and other toxic substances, which act as suicide in-activator of succinate dehydrogenase [2]. Various species of the genus *Indigofera* are used for various medicinal purposes. Traditionally, *I. daleoides* is used to cure diarrhea and considered effective againstseveral pathogens. *I. oblongifolia* was found to have antimicrobial [3], hepatoprotective [4]and lipoxygenase inihibition [5] activities. Chemical constituents of *I. pulchra* are effective neutralizer for snake-venom [3], whereas *I. tinctoria* possess free radical scavenging and anti-dyslipidemic activities [6]. The genus indigofera contain Plant sphingolipids a diverse group of lipids composed of polar head groups attached to CERs which contain SBs joined with FA moieties. The structural diversity, physiological roles, and metabolism of plant sphingolipids and glycosphingolipids are well documented [7, 8, 9, 10]. Extensive characterization of individual species in this complex and diversified class of plant lipids with powerful analytical tools led to the introduction of a new re-search area, sphingolipidomics [9]. Plant sphingolipids play critical roles in membrane stability and permeability, signaling, and cell regulation as well as cell-to-cell interactions [8, 10, 11] From the literature data reported above it is clear that this genus is

* Corresponding author.
E-mail address: muhammad_aurangzeb@hotmail.com (M. Aurang Zeb).

https://doi.org/10.1016/j.heliyon.2019.e02038
Received 18 July 2018; Received in revised form 24 February 2019; Accepted 1 July 2019

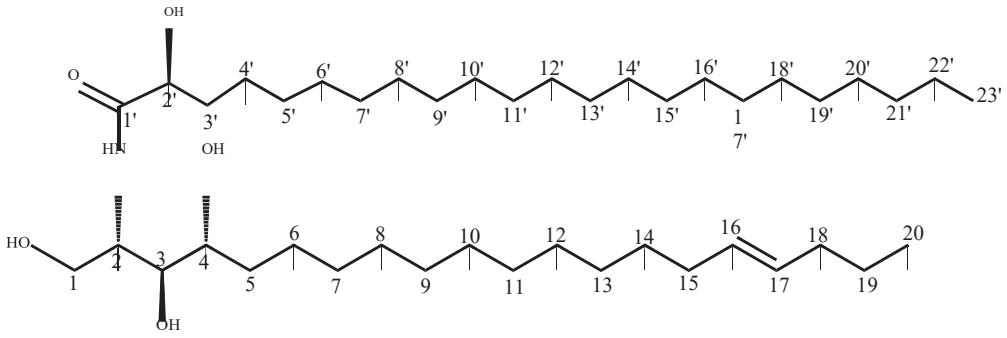

Fig. 1. Numbering scheme of indigoferamide A.

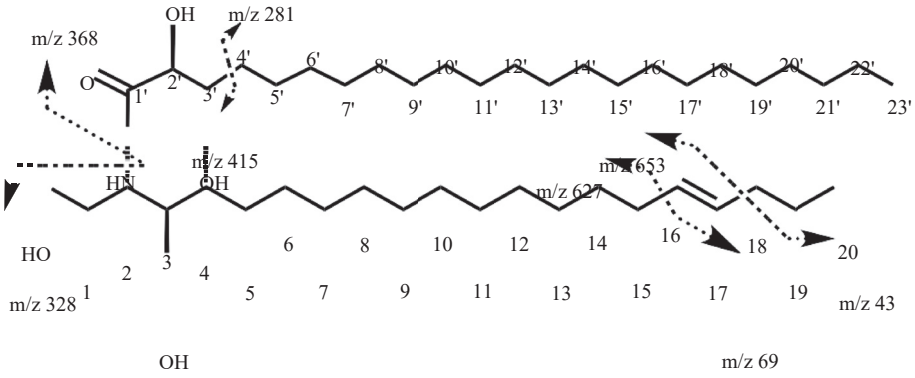

Fig. 2. Key EI MS fragmentation in indigoferamide A.

Table 1
^{1}H (600 MHz) and ^{13}C NMR (150 MHz) spectral data of indigoferamide A in MeOD.

C. No.	^{1}H NMR $_{H}$ (J in Hz)	^{13}C NMR $_{C}$	Multiplicity	HMBC
1	3.74, (d, J = 5)	62.0	CH_2	C-3
2	4.10, m	52.9	CH	C-1′
3	3.55, m	76.0	CH	–
4	3.52, m	73.2	CH	C-2, C-5
5	1.28, m	33.8	CH_2	–
6–7	1.28, m	27.2	CH_2	–
8–13	1.28, m	30.5	CH_2	–
14	1.28, m	33.7	CH_2	–
15	1.28, m	33.1	CH_2	–
16	5.43, m	131.6	CH	C-15
17	5.45, m	131.6	CH	–
18	1.28, m	32.7	CH_2	C-17
19	1.28, m	23.8	CH_2	–
20	0.89, (t, J = 7)	14.5	CH_3	C-18
1′	–	176.9	-C-	–
2′	4.02, m	72.9	CH	C-1′, C 3′
3′	1.61, m	35.8	CH_2	–
4′, 5′	1.28, m	30.5	CH_2	–
6′, 20’	1.28, m	30.5	CH_2	–
21’	1.28, m	33.8	CH_2	–
22’	1.28, m	23.8	CH_2	–
23’	0.89, (t, J = 7)	14.5	CH_3	–
NH	8.5, s	–	–	–

comprised of active therapeutic agents that are why the medicinal plant *I. heternatha* wall was selected to explore it phytochemically. In the current study, a novel indigoferamide-A, namely, (S)-2-hydroxy-N-((2S,3S, 4R,E)-1,3,4 trihydroxyicos-16-en-2-yl) tricosanamide, isolatedfrom *Indigofera heterantha* [12] was characterized by employing density functional theory calculations and molecular docking. In order to check the significance and medicinal potential of this novel compound it was subjected to various bioassays. These assays included anti-urease and antiglycation.

2. Material and methods

2.1. Plant material

The seeds of *Indigofera heterantha* were collected in May 2009 from Northern areas (Lower Dir) of Pakistan. The taxonomic identification of the plant was done by Department of Botany, Islamia College University, Peshawar, Pakistan. The voucher specimen (SJ-36) was deposited in the herbarium of the department.

2.2. Extraction and isolation

Shade-dried powdered seeds (22 kg) were extracted (thrice) with 5% aqueous methanol for seven days. The combined extract was evaporated under reduced pressure to get brownish residue F1 (2.29 kg), which was partitioned between chloroform and water to yield F2 (41 g, chloroform-soluble fraction) and F3 (1.6 kg, water-soluble fraction). The chloroform-soluble fraction (F2) was further partitioned into methanol and *n*-hexane fractions using Soxhlet extractor to afford FR1B (36 g) and FR1A (3 g), respectively. Water soluble fraction was also partitioned with ethyl acetate (EtOAc) to yield ethyl acetate soluble fraction FR3A (1 kg). FR3A was further subjected to fractionation using ether: petroleum ether (2:1) and water to get three fractions, FR3AC (400 g), FR3AB (160 g) and residue fraction FR3AA (360 g). The fraction FR3AC was subjected to column chromatography on silica gel and eluted with *n*-hexane- ethyl acetate in increasing polarity to yield six fractions (1–6). The fractions (3–5) were combined based on thin layer chromatography (TLC) profile and subjected to further column chromatography to yield 73 fractions. The mixed sub-fractions 41–64, were further chromatographed, and eluted with *n*-hexane-acetone in increasing polarity to obtain various sub-fractions. Further separation and purification of these fractions using pre-coated preparative TLC plates resulted in the isolation of one new compound.

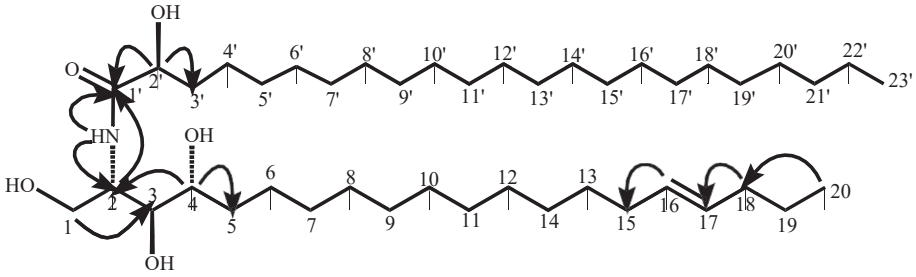

Fig. 3. Key HMBC correlations of indigoferamide A.

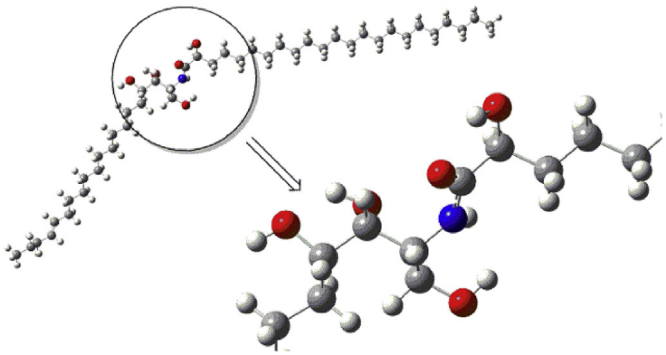

Fig. 4. Optimized geometry of indigoferamide A at B3LYP/6-31G(d,p).

Table 2
Selected optimized geometric parameters of indigoferamide A, calculated at B3LYP/6- 31G* in the gas phase (refer to Fig. 1 for numbering scheme).

Atoms	Bond lengths (Å)	Atoms	Angle (degrees)
C=O	1.23	O=C1-N	124.13
C-N	1.36	C15-C16-C17	125.47
C1'-O	1.42	C2-N-C1′	124.39
C2-O	1.43	Dihedral angles (degrees)	
C3-O	1.44	O-C4-C3-O	-57.62
C1'-O	1.41	O-C1-C2-N	-56.95
C=C	1.34	O=C-N-C	10.58
		O-C1-C1' = O	-12.98

2.3. Computational methods

All calculations were performed with Gaussian 09 [13]. The geometries were optimized without any symmetry constraints with B3LYP method using 6-31G (d,p) [14] basis set in the gas phase and in methanol. The B3LYP method consists of Becke's three-parameter hybrid functional [15] in conjunction with the correlation function of Lee, Yang, and Parr [16]. The B3LYP method is a cost-effective and accurate and works reasonably well for the prediction of geometries of a number of synthetic [17, 18, 19] and natural products [20, 21]. Conformational analysis has been performed with B3LYP/6-31G(d,p) without any symmetry constraints around three important dihedral angles; O=C-N-H, N-C2-C3-C4 and O-C2′-C3′-CC4' (See Figure SI-1, supporting information). The aliphatic chains were kept fully stretched during the conformational analysis. The minimum energy conformer was then fully optimized at B3LYP/6-31G(d,p) level of theory. The optimized structure was confirmed by frequency analysis at the same level (B3LYP/6-31G(d,p)) as a true minimum (without any imaginary frequency). The frequency analysis was performed in gas phase and in methanol solvent. Two scaling factors were applied because it is reported recently as an effective approach for accurate vibrational analysis [22]. ^{1}H and ^{13}C NMR calculations were performed in methanol solvent (MeOH) using GIAO/WP04/6-31 G (d, p) [23]. Polarization continuum model (PCM) [24] approach was applied to study the solvent effect. The reported theoretical chemical shifts are with respect to TMS as an internal standard. Although, the experimental UV-Vis did not reveal any peak in 200–800 nm range, but we have calculated the UV-Vis spectrum with TD-DFT/B3LYP/6-31G(d,p) in order to find the exact absorption maximum. The electronic properties such as electron affinity (E.A.), ionization potential (I.P), band gaps, coefficient of highest occupied molecular orbital (HOMO) and coefficient of lowest unoccupied molecular orbital (LUMO) are also calculated at B3LYP/6-31G(d,p). The band gap is taken as the difference in energies of HOMO and LUMO. Electronic properties such as hardness, softness, electronegativity is calculated from ionization potential and electron affinities using the following equations [25].

$$\text{Ionization potential (I.P.)} = -E_{HOMO}\ (\text{eV}) \quad (1)$$

$$\text{Electron affinity (E.A.)} = -E_{LUMO}\ (\text{eV}) \quad (2)$$

$$\text{Electronegativity (E.N.)} = (\text{I.P.} + \text{E.A.})/2\ (\text{eV}) \quad (3)$$

$$\text{Hardness } (\eta) = (\text{I.P.} - \text{E.A.})/2\ (\text{eV}) \quad (4)$$

$$\text{Softness (s)} = 1/(2\eta)\ (\text{eV}) \quad (5)$$

2.4. Urease inhibition assay

Reaction mixtures, consisting of 25 μL of enzyme (Jack bean ureases) solution and 55 μL of buffers containing 50 mM urea were incubated with 5 μL of test compound at 30 °C for 15 minutes in 96-well plates. Urease inhibition activity was determined by using the indophenol method [26]. Forty-five μL of phenol reagent (1% w/v phenol and 0.005% w/v sodium nitroprussside) and 70 μL of alkali reagent (0.5% w/v NaOH and 0.1% active sodium hypo chloride) were added. The assay was monitored by an increase in absorbance at 560 nm after 10 min, using a microplate reader (Molecular Devices, USA). All reactions were performed in triplicate in a final volume of 200 μL. The results (change in absorbance per minute) were processed by using SoftMax Pro software (Molecular Devices, USA). The assays were performed at pH 6.8. Percent (%) inhibition was calculated by formula 100- (OD test well/OD control) ×100. Thiourea was used as the standard inhibitor of urease.

2.5. In vitro antiglycation assay

In vitro antiglycation activity was examined by incubation of methylglyoxal (14 mM), different concentrations of test compounds (which are prepared in 10 % final DMSO concentration), NaN_3 (30 mM) in 0.1 M buffer solution (phosphate, pH 7.4), and BSA (10 mg/mL) under aseptic conditions for 9 days at 37 °C. Each sample was observed after 9 days against the sample blank for the specific fluorescence (excitation: 330 nm; emission: 440 nm) development [27]. The positive control was rutin. The % inhibition for each compound (formation of AGE) versus control was determined by using the following formula: % inhibition = (1-Fluorescence of test sample/Fluorescence of the control group) × 100 Rutin and methylglyoxal (MG) (40 % aqueous solution) were purchased

Table 3
Comparison of experimental and theoretical vibrational frequencies of indigoferamide in gas and methanol solvent and their assignment.

Wavenumber (Expt) cm^{-1}	Wavenumber (Unscaled) cm^{-1}	Wavenumber (Scaled) cm^{-1}	Wavenumber (Unscaled) cm^{-1}	Wavenumber (Scaled) cm^{-1}	Approximate Assignment
	Gas		Methanol		
	3838	3703	3828	3694	υ (OH)
3475	3804	3670	3796	3662	υ (OH)
	3780	3647	3761	3628	υ (OH)
	3640	3512	3633	3505	υ (OH)
3340	3626	3498	3620	3492	υ (NH)
	3124	3014	3121	3011	υ (CH)
	3112	3002	3118	3008	υ (CH_2)
	3111	3001	3108	2999	υ (CH_3)
	3110	3001	3106	2997	υ (CH_3)
	3106	2997	3103	2993	υ (CH_2-CH_3)
	3105	2996	3100	2991	υ (CH_2-CH_3)
	3096	2987	3095	2986	υ (CH_2)
	3093	2984	3089	2980	υ (CH_2)
2924	3079	2971	3086	2977	υ (CH_2) *Antisym.*
	3078	2970	3071	2963	υ (CH_2)
	3073	2965	3069	2961	υ (CH_2)
	3072	2964	3069	2961	υ (CH_2-CH_3)
	3063	2955	3060	2952	υ (CH_2)
	3058	2950	3051	2943	υ (CH_2)
	3038	2931	3039	2932	υ (CH_2)
	3037	2930	3037	2930	υ (CH_3)
	3030	2923	3029	2922	υ (CH_2)
	3027	2920	3028	2922	υ (CH_2)
2854	3004	2898	3006	2900	υ (CH_2)
	2991	2886	3003	2897	υ (CH) Aliphatic
	2981	2876	3002	2896	υ (CH) Aliphatic
1664	1748	1734	1729	1715	υ (C=O)
1664	1737	1723			υ (C=C)
	1552	1540	1563	1551	δ (NH), δ (CH)
	1459	1447	1446	1434	ω (CH_2) δ (OH)
	1451	1439	1435	1424	ω (CH_2) δ (OH)
	1436	1425			ω (CH_2)
	1404	1393	1402	1391	ω (CH_2)
	1323	1312	1318	1308	γ (CH_2) ρ(CH_2)
	1303	1293	1301	1290	γ (CH_2) υ (C-O)
	1296	1286	1298	1287	δ (OH), δ (CH)
	1233	1223	1230	1220	δ (OH), δ (CH)
	1120	1111	1115	1106	υ (CC), υ (CO)
	1092	1083	1086	1077	υ (CC), υ (CO))
	1084	1075	1082	1073	υ (CC), υ (CO)

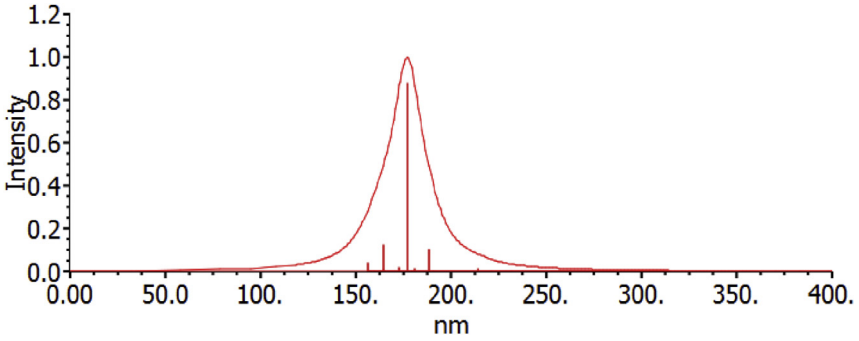

Fig. 5. Simulated UV Vis spectra of indigoferamide A in methanol, calculated at TD-DFT B3LYP/6-31G(d,p).

from Sigma-Aldrich (Japan), BSA (Bovine Serum Albumin) from Merck Marker (Germany), and disodium hydrogen phosphate (Na_2HPO_4), sodium azide (NaN_3) and sodium dihydrogen phosphate (NaH_2PO_4) from Scharlau Chemie, S. A. (Spain), while dimethyl sulphoxide (DMSO) was from Fischer Scientific (UK).

2.6. Molecular docking

To predict the bioactive conformations, the indigoferamide was docked into the binding pockets of the selected proteins (enzymes) by using the default parameters of MOE-Dock program. Before docking the ligands into protein molecules, MOE 2009-10 Build program (which is implemented in MOE) was used to sketch the isolated compound. Energy minimization was carried out up to 0.05 gradients by using MMFF94x force field through the default parameter of MOE energy minimization algorithm. The protein molecules of urease (PDB ID code: 4UBP) and α-glucosidase (PDB ID code: 3NO4) were downloaded from Protein Data Bank having resolutions of 1.55Å and 2.02Å respectively. All water molecules were removed from the receptor proteins and 3D protonation was carried out by using Protonate 3D Option. The energies of protein molecules were minimized by using the default parameters of MOE 2009-10 energy minimization algorithm (gradient: 0.05, Force Field:

Table 4
Wavelengths, energies and oscillator strengths of excitation in UV-Vis spectrum of indigoferamide A calculated at TD-DFT B3LYP/6-311G(d,p).

	nm	eV	Theoretical	Oscillator Strength (f_o)
1	188	6.57		0.1009
2	181	6.84		0.0125
3	177	6.99		0.8787
4	173	7.16		0.018
5	165	7.52		0.1243
6	156	7.92		0.436

MMFF94X). Then, all the ligands were docked into the binding pockets (selective residues/amino acids) of the above proteins using default parameters of MOE-Dock Program. Re-docking procedure was also applied to validate the accuracy of docking protocol [28]. After docking, all the complex images were analyzed for specific types of interactions; bond lengths and their 3D images were taken.

3. Results and discussions

3.1. Supporting spectral data of indigoferamide-A

Indigoferamide-A was earlier isolated as colorless powder [12]. The molecular formula $C_{43}H_{85}NO_5$ was inferred from HR-FABMS which showed molecular ion (Pseudo) $[M+H]^+$ peak at m/z 696.6806 (calcd. for $C_{43}H_{86}NO_5$; 696.6760) (Fig. 1). The structure was confirmed based on mass fragments (Fig. 2) in the EIMS at m/z 281 [M^+-$C_{23}H_{44}NO_5$], 368 [M^+-$C_{20}H_{39}O_3$], 223 [M^+-$C_{27}H_{55}NO_5$], 69 [M^+-$C_{38}H_{77}NO_5$] and 43 [M^+-$C_{40}H_{79}NO_5$]. Optical rotation of the compound was [α] ^{27}: -16. The IR spectrum exhibited absorption bands at 3475 (OH), 3340 (amide group), 1664 (C = O), 2924, 2854 cm^{-1} (aliphatic) which illustrated the presence of an amide fatty acid [29]. The ^{1}H NMR spectrum (Table 1) of Indigoferamide-A showed three oxygenated methine multiplet signals at δ_H3.55, 3.52 and 4.02 for H-3, H-4 and H-2', respectively, and a downfield nitrogenated methine multiplet at δ_H 4.10 for H-2. A doublet at δ_H 3.74 (J = 5 Hz, H-1) was assigned to the oxygen bearing methylene group. The two terminal methyl protons (H-20 and H-23′) appeared as triplets at δ_H 0.89 (J = 7 Hz, 6H). The characteristic resonances in the ^{1}H and ^{13}C NMR spectra (Table 1) at 176.9/8.56 (C-1′/N-H), 62.1/3.74 (C-1/H-1) and δ_C/δ_H 52.9/4.10 (C-2/H-2) confirmed the cerebroside skeleton [30]. The characteristic chemical shifts at δ_C 32.7–33.1 of the methylene carbons adjacent to the double bonds indicated the *E* geometry around the double bond (δ_C 26–28 for *Z*-geometry) [31, 32]. ^{1}H NMR spectrum was of little significane in assigning the *E*-stereochemistry due to the multiplets observed for H-16 and H-17. The NH proton (δ_H 8.56) showed HMBC correlation (Fig. 3) with carbonyl carbon (δ_C 176.9, C-1′) and a methine carbon (δ_C 52.9, C-2) which inidcated an amide linkage. The ^{1}H-^{1}H COSY correlation (Fig. 3) of indigoferamide-A can be

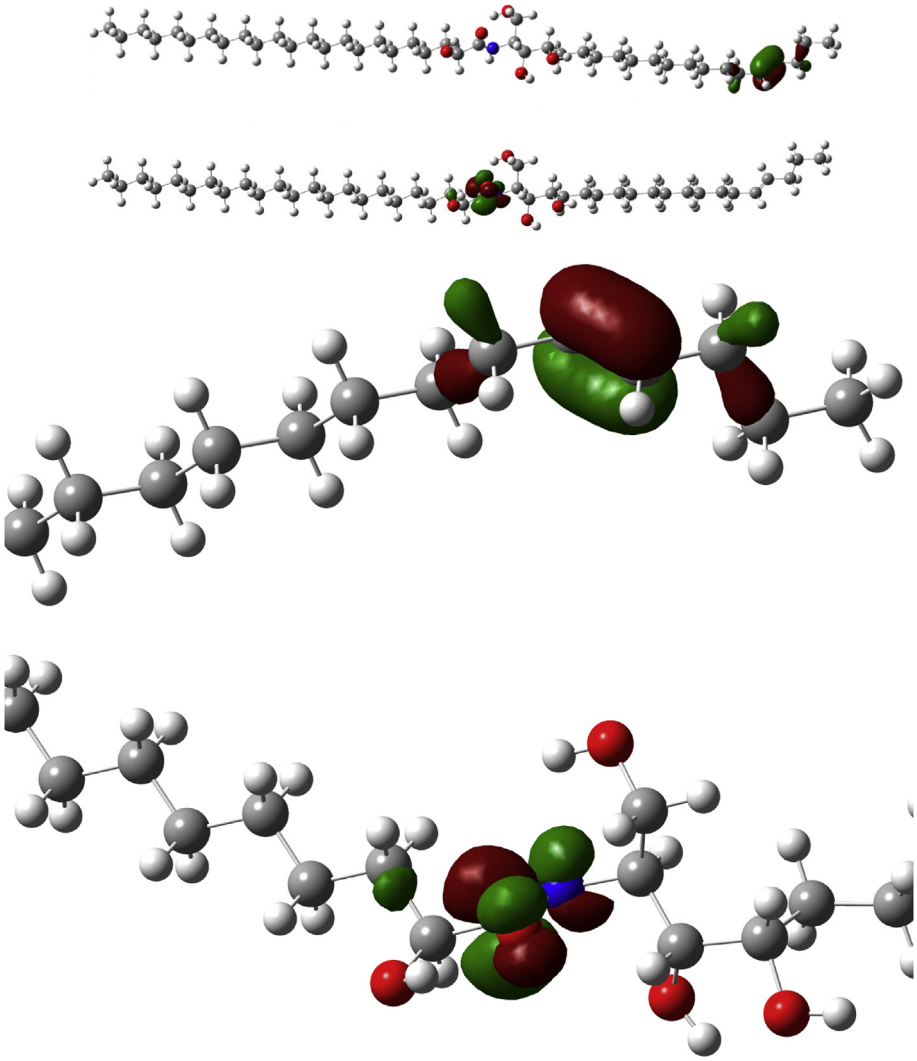

Fig. 6. HOMO and LUMO of indigoferamide A, calculated at B3LYP/6-31G(d,p). The orbitals are plotted at isodensity of 0.06.

Table 5
Comparative theoretical and experimental ^{1}H and ^{13}C NMR chemical shifts for indigoferamide A.

	^{1}H Chemical shifts (coupling constant)		^{13}C chemical shifts	
	Experimental	`Theoretical	Experimental	Theoretical
1	3.74, (d, $J = 5$)	3.96	62.0	60.99
2	4.10, m	3.28	52.9	66.40
3	3.55, m	4.95	76.0	72.98
4	3.52, m	1.85	73.2	76.30
5	1.28, m	1.65	33.8	31.32
6-7	1.28, m	1.60	27.2	30.12
8-13	1.28, m	1.60	30.5	34.7
14	1.28, m	1.73	33.7	35.26
15	1.28, m	2.23	33.1	37.68
16	5.43, m	5.90	131.6	125.38
17	5.45, m	5.82	131.6	125.99
18	1.28, m	2.35	32.7	38.56
19	1.28, m	1.73	23.8	28.95
20	0.89, (t, $J = 7$)	1.38	14.5	17.36
1′	–		176.9	170.84
2′	4.02, m	4.03	72.9	74.79
3′	1.61, m	1.57	35.8	41.82
4′, 5′	1.28, m	1.60	30.5	30.02,34.69
6′, 20’	1.28, m	1.60	30.5	34.6
21’	1.28, m	1.60	33.8	36.1
22’	1.28, m	1.60	23.8	26.96
23’	0.89, (t, $J = 7$)	1.38	14.5	18.26
NH	8.5, s		–	

Table 6
Urease activity exhibited by indigoferamide A.

S. No	Concentration (μM)	% Inhibition	IC_{50} (μM) ± S. E. M
(Indigoferamide A)	1000	29	323.21 ± 1.9
Thiourea	1000	83	21.01 ± 0.1

S. E. M. = Standard error of the mean of five assays * = Standard inhibitor for urease assay.

demonstrated as H-22′/H-23′, then H-2′/H-3′/H-4′and H-1/H-2/H-3/H-4/H-5/H-6. Comparison of ^{13}C NMR resonances with reported compounds helped in identifying the stereochemistry at chiral centers [33, 34].

3.2. Conformational analysis

DFT calculations have been performed to gain insight into the structure and spectroscopic properties of indigoferamide A. The correlation of the experimental and theoretical spectroscopic data supports the assigned structure. Conformation analyses have been performed at B3LYP/6- 31G(d,p). Three important dihedral angles were selected, and a series of conformers were obtained by rotation around these angles. First, different conformers were obtained at 10° rotation around O=C-N-H dihedral angle, and a plot of energies of conformers as a function of dihedral angle is shown in the supporting information (Fig. SI1). The lowest energy conformer was obtained at a dihedral angle of -177°. This rotation generates favourable nonbonding interaction of the hydrogen on C1 with the carbonyl oxygen. Next, the conformational analysis was performed by rotation around C2-C3 bond (NH-C2-C3-C4 dihedral angle). This rotation does not produce any conformer with the energy lower than the obtained from the above step (Fig. SI2). This rotation causes steric interaction between both aliphatic chains as they approach each other during the process. Next, rotation was performed around OH-C2′-C3′-C4′, and relative energy with respect to degree of rotation was analysed. The authors again could not locate any conformer with energy lower than the starting conformer (Fig. SI3). Some other important dihedral angles have been identified (for example, C2-C3- C4-C5); however, conformational analyses have not been performed around these bonds because such analyses would break the existing hydrogen bonding interactions and would definitely lead to increase in energy. Moreover, the aliphatic chains are fully stretched, and we had found that any rotation of the aliphatic chain (to form bent structure) would increase the energy of the conformer. The lowest energy conformer was fully optimized at B3LYP/6-31G(d,p). The geometry was also optimized in methanol and chloroform solvents. The optimized geometry is shown in (Fig. 4). C2-OH proton is a hydrogen bond donor to carbonyl oxygen at the distance of 1.94Å. The carbonyl oxygen also has nonbonding dipole type interactions with the hydrogen on C-3 (2.55Å). The amide nitrogen acts as a hydrogen bond acceptor from the hydroxyl on C1. Hydroxy moieties on C3 and C4 also have hydrogen bonding type interactions between them. The hydroxyl of C3 acts as a hydrogen bond donor to the oxygen of C4. Some important bond lengths and angles are shown in the (Table 2).

3.3. Infra-red spectral analysis

The experimental IR spectrum of indigoferamide A shows prominent peaks for olefinic C-H, aliphatic C-H, amide CO, alkene C=C stretching vibration in the functional group region as well as NH and C-H bending vibrations. The IR spectrum is also simulated at B3LYP/6-31G(d,p), and compared with the experimental spectrum. Two scaling factors are applied to the vibrational frequencies [22] for better correlation with the experimental results; frequencies above 1800 cm^{-1} are scaled with 0.9648 [35] whereas frequencies below 1800 cm^{-1} are scaled with 0.992. The amide NH stretching vibration is theoretically predicted to appear at 3492 cm^{-1}, which is slightly higher than the experimental 3340 cm^{-1}. This is probably attributed to the condensed phase nature of the molecules in the experimental IR spectrum. Two important simulated stretching vibrations of C- H bonds on olefinic moieties are; 3001 and 2996 cm^{-1}, for *anti*-symmetric and symmetric stretching of the alkene C-H bonds, respectively. The simulated C-H stretching vibrations for aliphatic protons were observed as a broad peak at 2990 cm^{-1}. The olefinic C=C and amide C=O stretching are simulated at 1680 and 1670 cm^{-1}. Both the vibrations were observed experimentally as a relatively broad peak at 1664 cm^{-1}, which shows the nice correlation between theoretical and experimental values. The N-H bending vibration was simulated at 1498 cm^{-1}, whereas the C-H bending vibrations at 1413 cm^{-1}. The C-O stretching vibrations are observed at 1252 cm^{-1}(Table 3).

3.4. UV-Vis analysis

The experimental UV-Vis analysis of the indigoferamide A did not reveal any absorption band above 200 nm which was consistent with the proposed structure of the compound. The UV-Vis spectra of indigoferamide A was simulated to find the position of the maximum wavelength of absorption. The theoretical spectrum was calculated in methanol solvent at TDDFT (B3LYP/6- 31G(d,p). The theoretical UV-Vis spectrum is shown in Fig. 5 whereas as wavelengths of excitations along with oscillator strength (*f*) are given in Table 4. Analysis of the orbitals indicate that the transition corresponds to π- π*. Analysis of the energies of molecular orbital reveals that the transition corresponding to λ_{max} is due to excitation from highest occupied molecular orbital (HOMO) to lowest unoccupied molecular orbital (LUMO).

The analysis of HOMO and LUMO (Fig. 6) shows that the charge density in HOMO is mainly localized on the olefinic moiety of indigoferamide A, whereas LUMO is localized on the amide part of the compound. HOMO to LUMO excitation is actually a charge transfer from olefin to amide moiety [36]. The HOMO LUMO gap was found to be 6.64 eV. This band gap is consistent with the excitation at 188 nm (6.57 eV). The high value of the band gap is indicative of the stability of the molecule. The energy of HOMO describes the ability of a compound to donate electron whereas the energy of the LUMO describes the ability of a compound to accept electron. Therefore, both HOMO and LUMO deliver useful information about oxidation and reduction abilities of the compound. The HOMO of indigoferamide A has energy of -6.44 eV,

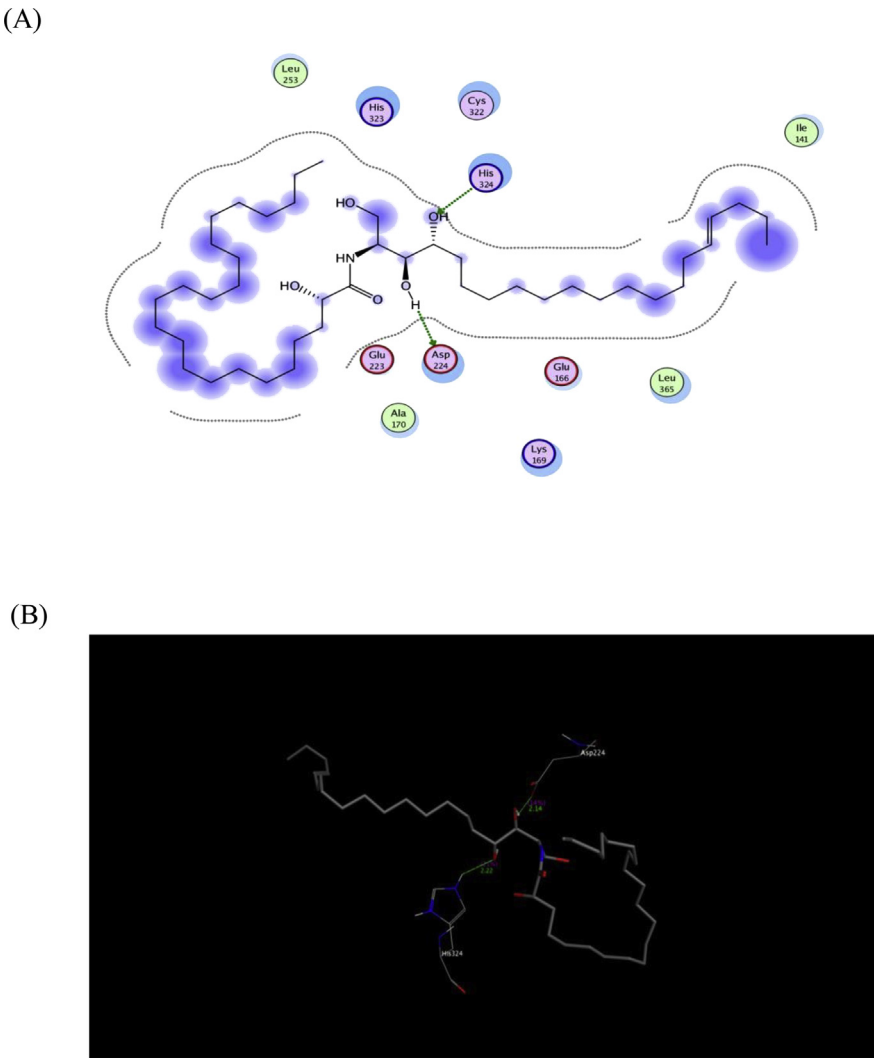

Fig. 7. 2D (A) and 3D (B) docking interaction images of indigoferamide A with the active pocket of urease.

Table 7
Antiglycation activity of indigoferamide A.

S. No	Compounds	Concentration (μM)	% Inhibition	IC50 (μM) ± S. E. M
1 (Indigoferamide A)	1	1000	40	NA
3. Rutin	2	1000	83	289.1 ± 0.3

S. E. M. = Standard error of the mean of five assays * = Standard inhibitor for antiglycation bioassay.

whereas the LUMO has energy of 0.2 eV. The very high value of HOMO illustrates the stability of the compound against oxidation [37]. The HOMO-LUMO band gap for the compound is 4.42 eV.

3.5. Electronic properties

We have calculated the electronic properties at B3LYP/6-31G(d,p) on the optimized geometry of indigoferamide A. Electronic properties are not studied experimentally for indigoferamide A, but they reveal useful information regarding stability and activities of a compound [27]. According to Koopmans theorem [38], energies of HOMO and LUMO can be approximately taken equivalent to ionization energy and electron affinity, respectively (vide supra). The HOMO in the compound has energy of -6.44 eV whereas the LUMO has energy of +0.20 eV which lead to the band gap of 6.64 eV. The very high band gap for the compound indicates its high stability. The ionization potential and electron affinities for the compound are 6.44 and -0.2 eV, respectively. Other electronic properties such as hardness, softness and electronegativity are calculated using the Eqs. (3), (4), and (5) given in the section of computational methods. Electronegativity, hardness and softness of the indigoferamide A are 3.32, 3.12 and 0.160 eV, respectively.

3.6. NMR analysis

The ^{1}H NMR spectrum of indigoferamide A was experimentally measured in MeOD on a 500 MHz spectrometer. The theoretical NMR is also calculated using Cramer re-parameterized WP04 functions at B3LYP/6-31G(d,p) in chloroform. The NMR was calculated using GIAO formalism, and the solvent effect was introduced through polarizable continuum model (PCM). NMR was calculated for all conformers lying within 2 kcal range of the minimum energy conformer, and the overall theoretical spectrum is Gaussian weighted average over all conformers. Although different conformers were taken into account; however, no significant differences could be observed between different conformers. A comparison of the theoretical ^{1}H and ^{13}C NMR chemical shifts with the experimental values is given in (Table 5). As it can be seen in the (Table 4), theoretical^{1}H NMR chemical shifts of the compound correlate nicely with the experimental chemical shifts without any scaling factor.

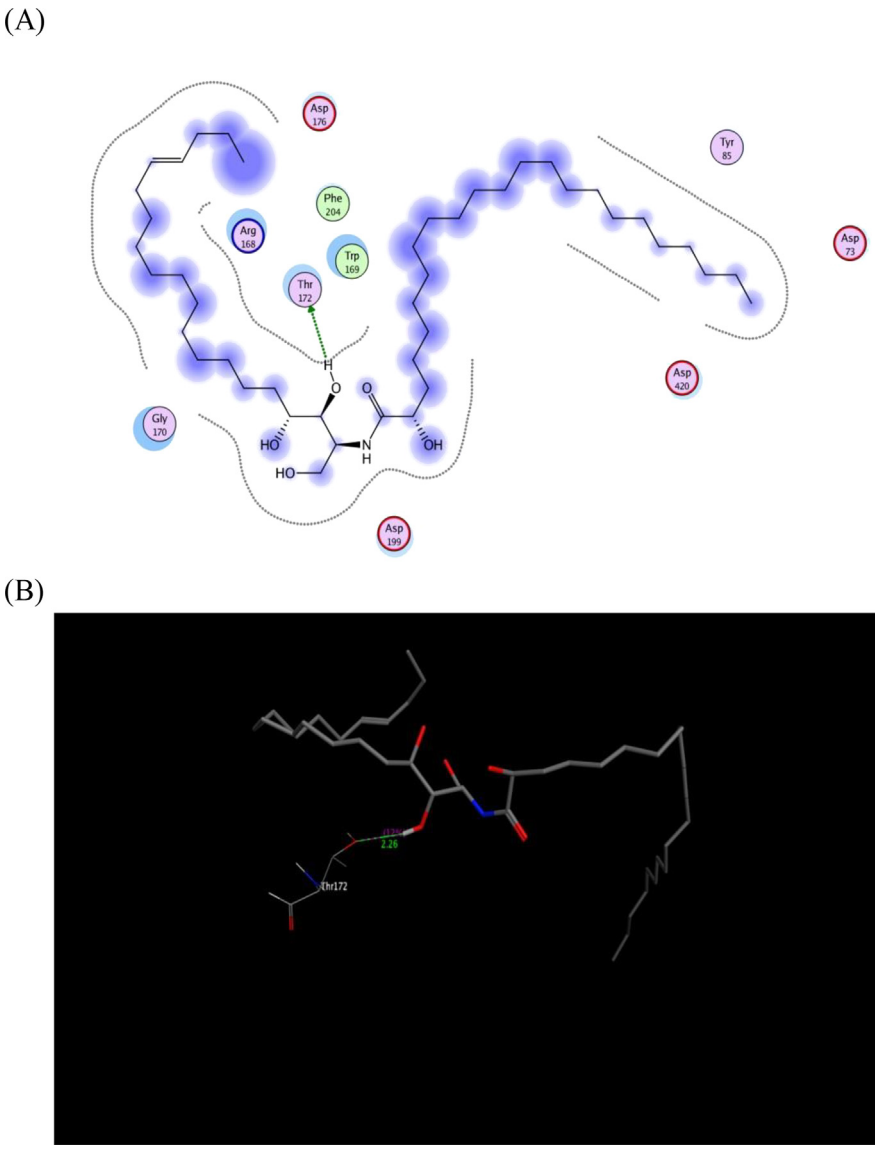

Fig. 8. 2D (A) and 3D (B) interaction images of indigoferamide A with the active pocket of Alpha glucosidase.

Similarly, the calculated ^{13}C NMR chemical shifts of indigoferamide A also correlate adequately with the experimental chemical shift values.

3.7. Urease activity

Urease plays significant role in plant nitrogen metabolism [36, 37]. Urease has been recognized as a virulence factor as it participates in the development of kidney stones, pyelonephritis, peptic ulcers, and other diseases [39, 40]. The search of effective and safe urease inhibitors is very important area of pharmaceutical research [41, 42, 43]. In continuation of our efforts to discover new and potent inhibitors of medicinally important enzymes through high-throughput screening assays, we identified this compound, having considerable efficacy against ureases (Table 6). From the docking results it was clear that the indigoferamide was strongly bound in the active site of urease by making two strong interactions with His324 and Asp224 amino acid residues as shown in (Fig. 7). The first strongest side chain donor interaction was found between His324 and OH group of the long chain with a bond distance of 2.14 angstrom. Asp224 showed strong side chain accepter interaction with hydrogen atom of OH group of long chain having a bond length of 2.22 angstrom. Some other residues like Glue166, Glu223 and His323 were also present in the nearby vicinity.

3.8. Antiglycogen activity

The same compound was docked into the binding pockets of α-glucosidase. The compound showed promising antiglycogen activity (Table 7). From the 2D and 3D interaction images, it was clear that Thr172 showed a strong single side chain acceptor interaction with OH group of the long hydrocarbon chain of the indigoferamide. It has given a bond distance of 2.26 Å as shown in the (Fig. 8). Trp169, Arg168 and Gly170 were also present in the nearest region.

4. Conclusions

The indigoferamide-A, isolated from *Indigofera heterantha* was characterized by modern spectroscopic analytical techniques. DFT calculations of the compound have been performed at B3LYP/6-31G(d,p) level for obtaining geometries and spectroscopic properties of indigoferamide-A. Conformational analyses have been performed to locate the lowest energy conformer. The vibrational spectrum of the compound, simulated at B3LYP/6-31G (d,p) shows nice correlation with the experimental IR spectrum through a scaling factor of 0.9648. Analysis of UV-Vis spectrum and HOMO and LUMO illustrated that the transition corresponding to the maximum wavelength is a transition from HOMO to LUMO. ^{1}H and ^{13}C

NMR was calculated using Cramer's reparameterized function WP04 at 6-31G(d,p) basis set. Although different conformers were considered for the calculation of chemical shifts; however, no significant differences were observed among these conformers. Electronic properties such as band gap, ionization potential, electronegativity, electron affinities, softness and hardness were also simulated for the first time; however, no comparison could be made with the experiment. The indigoferamide A was screened for urease and antiglycation activities. The compound showed good activity against urease enzyme. Molecular docking simulations reveal useful information regarding the binding of indigoferamide-A with the urease enzyme.

Declarations

Author contribution statement

Taj Ur Rahman, Tariq Mahmood, Muhammad Sajid, Riaz Hussain: Performed the experiments.

Muhammad Aurang Zeb: Performed the experiments; Wrote the paper.

De-Bing Pu: Analyzed and interpreted the data.

Wajiha Liaqat: Contributed reagents, materials, analysis tools or data.

Khurshid Ayub: Performed the experiments; Analyzed and interpreted the data.

Wei-Lie Xiao: Conceived and designed the experiments.

Funding statement

This research did not receive any specific grant from funding agencies in the public, commercial, or not-for-profit sectors.

Competing interest statement

The authors declare no conflict of interest.

Additional information

Supplementary content related to this article has been published online at https://doi.org/10.1016/j.heliyon.2019.e02038.

References

[1] AliSI, Flora of Pakistan, Karachi, 1977.
[2] A. Malik, N. Riaz, H. Ahmad, S.A. Nawaz, M.I. Choudhary, Lipoxygenase inhibiting constituents from Indigofera hetrantha. Chem. Pharm. Bull. 53 (3) (2005) 263–266.
[3] M.U. Dahot, Antibacterial and antifungal activity of small protein of Indigofera oblongifolia leaves, J. Ethnopharmacol. 64 (3) (1999) 277–282.
[4] M. Shahjahan, G. Vani, C.S. Devi, Protective effect of Indigofera oblongifolia in CCl4-induced hepatotoxicity, J. Med. Food 8 (2) (2005) 261–265.
[5] A. Sharif, E. Ahmed, A. Malik, N. Riaz, N. Afza, S.A. Nawaz, M.I. Choudhary, Lipoxygenase inhibitory constituents fromIndigofera oblongifolia, Arch. Pharm. Res. 28 (7) (2005) 761–764.
[6] D. Prakash, S. Suri, G. Upadhyay, B.N. Singh, Total phenol, antioxidant and free radical scavenging activities of some medicinal plants, Int. J. Food Sci. Nutr. 58 (1) (2007) 18–28.
[7] P. Sperling, E. Heinz, Plant sphingolipids: structural diversity, biosynthesis, first genes and functions, Biochim. Biophys. Acta 1632 (1-3) (2003) 1–15.
[8] S. Spassieva, J. Hille, Plant sphingolipids today-are they still enigmatic? Plant Biol. 5 (02) (2003) 125–136.
[9] M.O. Pata, Y.A. Hannun, C.K.Y. Ng, Plant sphingolipids: decoding the enigma of the Sphinx, New Phytol. 185 (3) (2010) 611–630.
[10] D.V. Lynch, T.M. Dunn, An introduction to plant sphingolipids and a review of recent advances in understanding their metabolism and function, New Phytol. 161 (3) (2004) 677–702.
[11] D. Warnecke, E. Heinz, Recently discovered functions of glucosylceramides in plants and fungi, Cell. Mol. Life Sci. 60 (5) (2003) 919–941.
[12] T.U. Rahman, M. Arfan, W. Liaqat, G. Uddin, M.I. Choudhary, Isolation of a novel indigoferamide-A from seeds of indigofera heterantha wall and its antibacterial activity, Records Nat. Prod. 8 (4) (2014) 412.
[13] M.J. Frisch, G.W. Trucks, H.B. Schlegel, G.E. Scuseria, M.A. Robb, J.R. Cheeseman, G. Scalmani, V. Barone, B. Mennucci, G.A. Petersson, H. Nakatsuji, M. Caricato, X. Li, H.P. Hratchian, A.F. Izmaylov, J. Bloino, G. Zheng, J.L. Sonnenberg, M. Had, Gaussian 09 Rev C.01, Gaussian Inc., Wallingford, CT, 2010.
[14] P.C. Hariharan, J.A. Pople, The influence of polarization functions on molecular orbital hydrogenation energies, Theor. Chim. Acta 28 (1973) 213–222.
[15] A.D. Becke, Becke's three parameter hybrid method using the LYP correlation functional, J. Chem. Phys. 98 (1993) 5648–5652.
[16] C. Lee, W. Yang, R.G. Parr, Development of the Colle-Salvetti correlation-energy formula into a functional of the electron density, Phys. Rev. B 37 (2) (1988) 785.
[17] T.Q. Hung, N.N. Thang, T.T. Dang, K. Ayub, A. Villinger, A. Friedrich, P. Langer, Palladium catalyzed synthesis and physical properties of indolo [2, 3-b] quinoxalines, Org. Biomol. Chem. 12 (32) (2014) 6151–6166.
[18] I. Javed, A. Khurshid, M.N. Arshad, Y. Wang, Photophysical and electrochemical properties and temperature dependent geometrical isomerism in alkyl quinacridonediimines, New J. Chem. 38 (2) (2014) 752–761.
[19] H. Ullah, A.U.H.A. Shah, K. Ayub, S. Bilal, Density functional theory study of poly (o-phenylenediamine) oligomers, J. Phys. Chem. C 117 (8) (2013) 4069–4078.
[20] H. Ullah, A. Rauf, Z. Ullah, M. Anwar, G. Uddin, K. Ayub, Density functional theory and phytochemical study of Pistagremic acid, Spectrochim. Acta Mol. Biomol. Spectrosc. 118 (2014) 210–214.
[21] M.A. Hashmi, A. Khan, K. Ayub, U. Farooq, Spectroscopic and density functional theory studies of 5, 7, 3′, 5′-tetrahydroxyflavanone from the leaves of Olea ferruginea, Spectrochim. Acta Mol. Biomol. Spectrosc. 128 (2014) 225–230.
[22] S. Mishra, P. Tandon, DFT study of structure and vibrational spectra of ceramide 3: comparison to experimental data, Mol. Simul. 38 (11) (2012) 872–881.
[23] K.W. Wiitala, T.R. Hoye, C.J. Cramer, Hybrid density functional methods empirically optimized for the computation of 13C and 1H chemical shifts in chloroform solution, J. Chem. Theory Comput. 2 (4) (2006) 1085–1092.
[24] J. Tomasi, B. Mennucci, R. Cammi, Quantum mechanical continuum solvation models, Chem. Rev. 105 (8) (2005) 2999–3094.
[25] J.I. Martínez-Araya, G. Salgado-Morán, D. Glossman-Mitnik, Computational Nanochemistry Report on the Oxicams–Conceptual DFT Indices and Chemical Reactivity, The J. Phys. Chem. B 117 (21) (2013) 6339–6351.
[26] M. Dixon, The determination of enzyme inhibitor constants, Biochem. J. 55 (1953) 170.
[27] C. Lee, M.B. Yim, P.B. Chock, H.S. Yim, S.O. Kang, Oxidation-reduction properties of methylglyoxal-modified protein in relation to free radical generation, J. Biol. Chem. 273 (39) (1998) 25272–25278.
[28] J. Boström, J.R. Greenwood, J. Gottfries, Assessing the performance of OMEGA with respect to retrieving bioactive conformations, J. Mol. Graph. Model. 21 (5) (2003) 449–462.
[29] M.U. Dahot, Antibacterial and antifungal activity of small protein of Indigofera oblongifolia leaves, J. Ethnopharmacol. 64 (3) (1999) 277–282.
[30] V.U. Ahmad, J. Hussain, H. Hussain, U. Farooq, E. Akber, S.A. Nawaz, M.I. Choudhary, Two Ceramides from Tanacetum artemesioides, Naturforsch Z 59b (2004) 329–333.
[31] S. Zareen, M.I. Choudhary, M.N. Akhtar, F.N. Ngounou, A triterpenoidal saponin and sphingolipids from Pteleopsis hylodendron, Phytochemistry 69 (12) (2008) 2400–2405.
[32] Z. Gao, Z. Ali, I.A. Khan, Glycerogalactolipids from the fruit of Lycium barbarum, Phytochemistry 69 (16) (2008) 2856–2861.
[33] J.D. Wansi, J.L.D Bavoua, E.N. Happi, K.P. Devkota, B.N. Lenta, M.A. Mesaik, M.I. Choudhary, Z.T. Fomum, N. Sewald, Bioactive Phenylethanoids and Coumarines from Basalmocitrus cameroonensis, Z. Naturforsch. 64b (2009) 452–458.
[34] S. Kawatake, K. Nakamura, M. Inagaki, R. Higuchi, Isolation and structure determination of six glucocerebrosides from the starfish Luidia maculata, Chem. Pharm. Bull. 50 (8) (2002) 1091–1096.
[35] J. Casado, V. Hernández, F.J. Ramirez, J.T. López Navarrete, Ab initio HF and DFT calculations of geometric structures and vibrational spectra of electrically conducting doped oligothiophenes, J Mol Struct (Theochem) 463 (1999) 211–216.
[36] L. Xiao-Hong, C. Hong-Ling, Z. Rui-Zhou, Z. Xian-Zhou, Theoretical investigation on the non-linear optical properties, vibrational spectroscopy and frontier molecular orbital of (E)-2-cyano-3-(3-hydroxyphenyl) acrylamide molecule, Spectrochim Acta A Mol Biomol Spectrosc 137 (2014) 321–327.
[37] F. Ian, Molecular Orbitals and Organic Chemical Reactions, Wiley-VCH Verlag GmbH, 2009.
[38] T. Koopmans, Über die Zuordnung von Wellenfunktionen und Eigenwerten zu den einzelnen Elektronen eines Atoms, Physica 1 (1-6) (1934) 104–113.
[39] H.L. Mobley, R.P. Hausinger, Microbial ureases: significance, regulation, and molecular characterization, Microbiol. Mol. Biol. Rev. 53 (1) (1989) 85–108.
[40] E. Bayerdörffer, R. Ottenjann, The role of antibiotics in Campylobacter pylori associated peptic ulcer disease, Scand. J. Gastroenterol. 23 (sup142) (1988) 93–100.
[41] Z. Amtul, R.A. Siddiqui, M.I. Choudhary, Chemistry and mechanism of urease inhibition, Curr. Med. Chem. 9 (14) (2002) 1323–1348.
[42] Z. Amtul, M. Rasheed, M.I. Choudhary, S. Rosanna, K.M. Khan, Kinetics of novel competitive inhibitors of urease enzymes by a focused library of oxadiazoles/thiadiazoles and triazoles, Biochem. Biophys. Res. Commun. 319 (2004) 1053–1063.
[43] V.U. Ahmad, J. Hussain, H. Hussain, A.R. Jasshi, F. Ullah, M.A. Lodhi, A. Yasin, M.I. Choudhary, First natural urease inhibitor from Euphorbia decipiens, Chem. Pharm. Bull. 51 (2003) 719–723.